Inorganic Chemistry

Article

pubs.acs.org/IC

Modulating Magnetic Dynamics of Dy_2 System through the Coordination Geometry and Magnetic Interaction

Peng Zhang,[†,‡] Li Zhang,[†,§] Shuang-Yan Lin,[†,‡] Shufang Xue,[†,‡] and Jinkui Tang*[,†]

[†]State Key Laboratory of Rare Earth Resource Utilization, Changchun Institute of Applied Chemistry, Chinese Academy of Sciences, Changchun 130022, People's Republic of China

[‡]University of Chinese Academy of Sciences, Beijing 100039, People's Republic of China

[§]College of Chemistry and Chemical Engineering, Inner Mongolia University, Hohhot 010021, People's Republic of China

Supporting Information

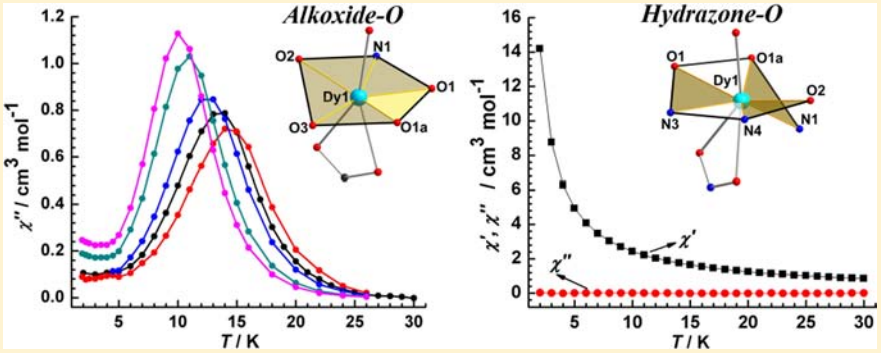

ABSTRACT: Two new dinuclear dysprosium compounds, $[Dy_2(HL_1)_2(PhCOO)_2(CH_3OH)_2]$ (**1**) and $[Dy_2(L_2)_2(NO_3)_2(CH_3OH)_2]\cdot 2CH_3OH\cdot 4H_2O$ (**2**), have been assembled through applying two ligands with different coordination pockets. The different features of ligands H_3L_1 and H_2L_2 result in the distinct coordination geometry of the metal ions in their respective structures. The Dy ions of complexes **1** and **2** were linked by the alkoxide- and hydrazone-O, and display the hula hoop-like and the broken hula hoop-like coordination geometry, respectively. Consequently, these two compounds show distinct magnetic properties. Complex **1** behaves as a single molecule magnet (SMM) with rather slow quantum tunneling rate ($\tau > 274$ ms), while no SMM behavior was observed for complex **2**. In addition, the comparison of the structural parameters among the similar Dy_2 SMMs with hula hoop-like geometry reveals the significant role played by coordination geometry and magnetic interaction in modulating the relaxation dynamics of SMMs.

INTRODUCTION

Since the seminal discovery of single molecule magnet (SMM) behavior in a Mn_{12} complex during the 1990s, the study of SMM has been the focus of chemistry, physics, and materials science, where the quantum world of magnetization for single molecule clusters meets the bulk scale of classical physics.[1−4] The continued interest stems from their prospects of applications in information storage and quantum computing.[5] In particular, recent years have seen a flurry of results for lanthanide-based SMMs, including the highest relaxation energy barriers for multinuclear clusters[6] and the highest blocking temperature,[7] which mainly benefit from the significant magnetic anisotropy of lanthanide ions arising from the large, unquenched orbital angular momentum.[8,9] Remarkably, the alteration of coordination geometry on local metal sites and/or magnetic interaction between them turns out to be a key factor in modulating the relaxation dynamics of lanthanide-based SMMs.[10−13] The high axial coordination geometry around Dy^{III} ions is an important feature enabling lanthanide complexes functioning as SMMs with high barrier, such as the approximate D_{4d} symmetry in $[LnPc_2]$[14,15] and the axial hula hoop-like geometry in asymmetric Dy_2[16] and Dy_6 triangular prism.[17] In addition, the tune of magnetic interactions can also bring about some surprising results, although exchange coupling between lanthanide metal centers is very weak.[16,18] To date, extensive research attempts have been performed to probe how the exchange coupling affects SMM properties in lanthanide-based complexes, thus yielding a series of ground-breaking results, such as the high blocking temperature discovered in N_2^{3-}-bridged Tb_2 complex and sulfur-bridged organometallic dysprosium complexes.[7,12]

Herein, to investigate the effects of magnetic interaction and coordination geometry on the SMM behavior in Dy-based compounds with hula hoop-like geometry, we employed two ligands with different features, H_3L_1[19−21] and H_2L_2 (Scheme 1), and obtained two novel Dy_2 compounds, $[Dy_2(HL_1)_2(PhCOO)_2(CH_3OH)_2]$ (**1**) and $[Dy_2(L_2)_2(NO_3)_2$-

Received: January 21, 2013
Published: March 25, 2013

   dx.doi.org/10.1021/ic400150f | Inorg. Chem. 2013, 52, 4587−4592

Scheme 1. Schematic Diagram of Ligands Used in Compounds 1, 2, 3, and 4

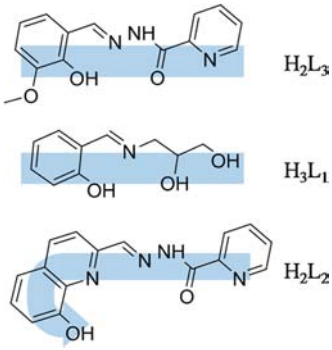

$(CH_3OH)_2]\cdot 2CH_3OH\cdot 4H_2O$ (**2**), from such ligands. The two compounds show the different structures concomitant with the observation of distinct static and dynamic magnetism. Further, the structure−property relationship can be revealed by the comparisons of four Dy_2 complexes containing two complexes from vanillin picolinoylhydrazone ligands.

EXPERIMENTAL SECTION

General Information. All chemicals were used as received without any further purification, and all manipulations were performed under aerobic conditions. Elemental analysis (C, H, and N) were carried out on a Perkin-Elmer 2400 analyzer. IR spectra were recorded with a Perkin-Elmer Fourier transform infrared spectrophotometer with samples prepared as KBr disks in the 4000−300 cm^{-1} range. Magnetic susceptibility measurements were obtained in the temperature range 2−300 K, using a Quantum Design MPMS XL-7 SQUID magnetometer equipped with a 7 T magnet. The experimental magnetic data are corrected for the diamagnetism estimated from Pascal's constants[22] and sample holder calibration.

X-ray Crystallographic Analysis and Data Collection. Single-crystal X-ray data of the title complexes were collected at 273(2) K on a Bruker Apex II CCD diffractometer equipped with graphite-monochromatized Mo Kα radiation (λ = 0.71073 Å). Data processing was completed with the SAINT processing program. The structure was solved by direct methods and refined by full matrix least-squares methods on F_2 using SHELXTL-97.[23] The locations of the Dy atoms were easily determined, and C, O, and N atoms were determined from the difference Fourier maps. The nonhydrogen atoms were refined anisotropically. All hydrogen atoms were introduced in calculated positions and refined with fixed geometry with respect to their carrier atoms.

Synthesis of $[Dy_2(HL_1)_2(PhCOO)_2(CH_3OH)_2]$ (**1**). Ligand $H_3\mathbf{L}_1$ (0.1 mmol) was dissolved in CH_3OH/CH_3CN (10 mL/5 mL) followed by the addition of $Dy(PhCOO)_3\cdot 6H_2O$ (0.1 mmol) and triethylamine (0.2 mmol), which gave a clear pale-yellow solution after stirring for 2 h. Diethyl ether was allowed to diffuse slowly into this solution at room temperature, and yellow single crystals were obtained in 1 week in 52% yield (26 mg). Anal. Calcd for $C_{36}H_{40}Dy_2N_2O_{12}$: C, 42.49; H, 3.96; N, 2.75. Found: C, 42.07; H, 3.65; N, 2.47. IR (KBr, cm^{-1}): 3641 (m), 3196 (br), 2894 (m), 2839 (m), 2666 (w), 1630 (s), 1595 (s), 1537 (s), 1494 (m), 1470 (s), 1423 (s), 1344 (s), 1325 (m), 1248 (m), 1219 (w), 1192 (m), 1150 (m), 1121 (s), 1042 (m), 1030 (s), 936 (w), 886 (m), 864 (m), 824 (w), 757 (m), 721 (s), 688 (m), 627 (s), 595 (m), 527 (s), 504 (m).

Synthesis of $[Dy_2(L_2)_2(NO_3)_2(CH_3OH)_2]\cdot 2CH_3OH\cdot 4H_2O$ (**2**). Ligand $H_2\mathbf{L}_2$ (0.1 mmol) was dissolved in a mixed solvent of CH_3OH/CH_3CN (5 mL/10 mL) followed by the addition of $Dy(NO_3)_3\cdot 6H_2O$ (0.1 mmol) and triethylamine (0.2 mmol), which gave a clear red solution after stirring for 3 h. This solution was left unperturbed to allow the slow evaporation of the solvent. After 4 days, red block-shaped crystals were formed in 38% yield (23 mg). Anal. Calcd for $C_{36}H_{44}Dy_2N_{10}O_{18}$: C, 35.15; H, 3.60; N, 11.38. Found: C, 34.71; H,

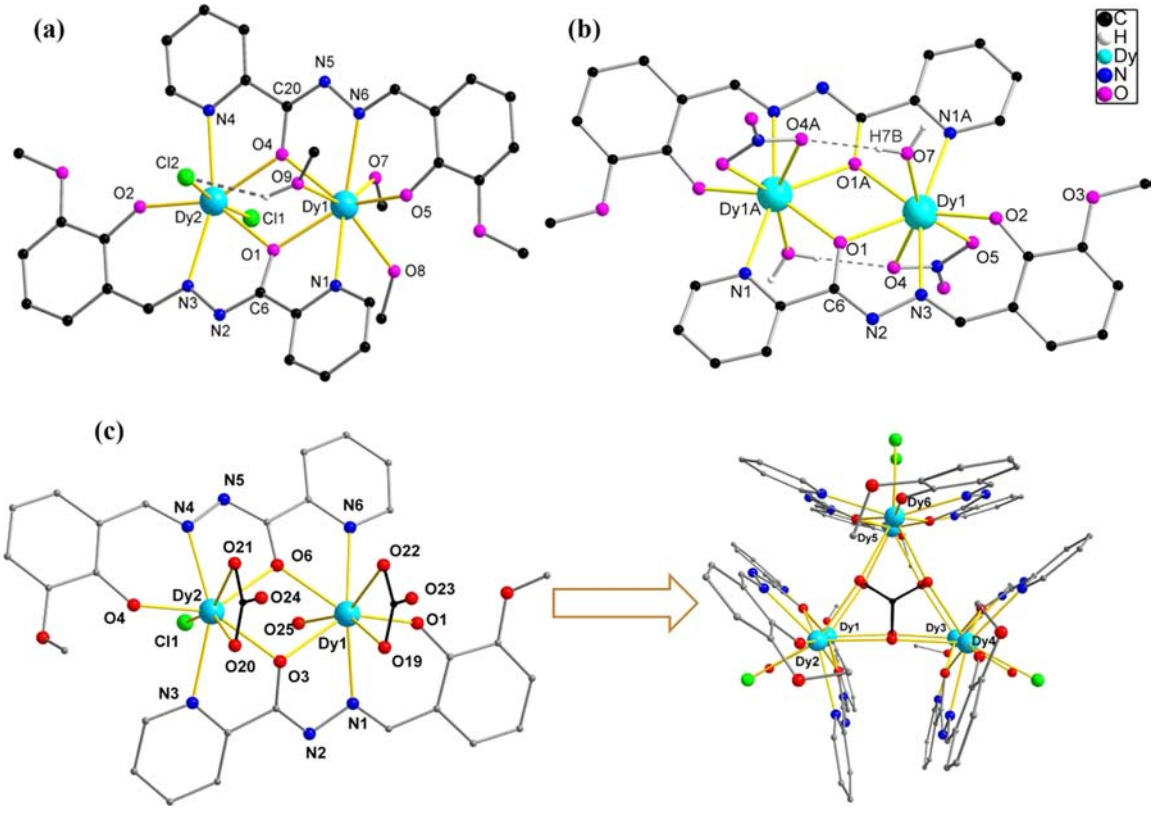

Figure 1. The crystal structures of compounds from ligand H_2L_3 (**3**, **4**, and Dy_6). Adapted from refs 16, 13, and 17.

dx.doi.org/10.1021/ic400150f | Inorg. Chem. 2013, 52, 4587−4592

3.15; N, 11.17. IR (KBr, cm^{-1}): 3402 (br), 1633 (w), 1590 (s), 1548 (m), 1499 (s), 1475 (s), 1449 (s), 1433 (m), 1384 (s), 1340 (s), 1308 (s), 1255 (w), 1169 (w), 1106 (s), 1049 (m), 1012 (w), 973 (w), 944 (w), 922 (m), 904 (m), 839 (m), 768 (m), 753 (m), 742 (m), 716 (m), 692 (m), 653 (m), 489 (m).

RESULTS AND DISCUSSION

For ligand H_2L_3, two Dy_2 compounds (Figure 1, asymmetric Dy_2 (**3**)[16] and centrosymmetric Dy_2 (**4**)[13]) with hula hoop-like geometry have been reported by our group, which both show the typical SMM behavior. In particular, the asymmetric Dy_2 compound (**3**) shows the high axiality and strong Ising exchange interaction, which efficiently suppresses quantum tunneling of the magnetization. Furthermore, the assembly of Dy_2 unit leads to a novel Dy_6 SMM with triangular prism arrangement (Figure 1c), indicating that such Dy_2 compounds with hula hoop-like geometry are useful building blocks for constructing new Dy-based SMMs.[17] As compared to ligand H_2L_3, ligand H_3L_1 provides similar coordination sites (two close coordination pockets showing a linear arrangement), whereas a clear difference was observed in the part of aldehyde for hydrazone ligand H_2L_2, as shown in Scheme 1. Therefore, compound **1** displays similar hula hoop-like coordination geometry around each Dy ion, while such geometry is broken in compound **2** due to the bent nature of H_2L_2 ligand. Detailed magnetization dynamics studies reveal typical SMM behavior for compound **1**, but no SMM properties for compound **2** probably due to the changes of coordination geometry of dysprosium ions and/or interactions between them. In addition, compound **1** represents the rare alkoxide-O bridged Dy_2 complex that behaves as a SMM. Notably, until now the Dy-SMMs based on alkoxide bridging ligand ($R-O^-$) are still rare for the lanthanide complexes with small-nuclearity ($n < 5$).[24−27]

Crystal Structures of 1 and 2. The reaction of $Dy(PhCOO)_3{\cdot}6H_2O$ with H_3L_1 in 2:1 CH_3OH/CH_3CN in the presence of triethylamine followed by Et_2O diffusion leads to the formation of pale-yellow crystals of **1**, while compound **2** was obtained by the reaction of $Dy(NO_3)_3{\cdot}6H_2O$ with H_2L_2 in 1:2 CH_3OH/CH_3CN in the presence of triethylamine. Crystal data and structure refinement details for **1** and **2** are summarized in Table 1. Their crystal structures have been depicted in Figure 2. Compounds **1** and **2** crystallize in the triclinic $P\bar{1}$ and orthorhombic *Pnna* space group, respectively.

In compound **1**, two Dy^{III} ions are bridged by the μ-$O_{alkoxide}$ atoms from two ligands, with Dy−O bond lengths of 2.295(2) and 2.261(0) Å, Dy···Dy distance of 3.769(9) Å, as well as Dy−O−Dy angle of 111.66(9)° (Figure 2a). Here, eight-coordinate Dy1 center demonstrates a hula hoop-like coordination geometry with the cyclic ring defined by the atoms N1, O1, O1a, O3, and O2 from two ligands (Figure 3a), which resembles that in compounds **3** and **4**. In general, the "hula hoop" configuration may favor persistent axiality of Dy ions, and the orientations of easy axes will further affect the dipolar−dipolar magnetic interactions within the molecule. In addition, one $PhCOO^-$ and one CH_3OH are coordinated to each dysprosium ion, completing the coordination sphere around it. Furthermore, in the crystal of compound **1**, the strong intra- and intermolecular hydrogen-bonding interactions result in a one-dimensional supramolecular chain similar to that in complex **3** (Figure S1).

In contrast, compound **2** displays a μ-$O_{hydrazone}$ bridged Dy_2 metal core, with Dy−O/N distances in the range of 2.290(6)−2.575(6) Å and Dy−O−Dy angle of 114.9(2)° (Figure 2b). The two ligands bind two Dy^{III} ions in a spiral twisted "head-to-tail" fashion with the quadridentate (O1, O2, N3, and N4) and bidentate (O1a, N1) unit (Figure 2b). A closer look at the crystal structure of **2** reveals the broken hula hoop-like coordination geometry on Dy^{III} sites, as seen in Figure 3b, which should arise from the different features of ligand H_2L_2 from H_2L_3. The bend of ligand H_2L_2 leads to the distortion of the structure, thus breaking the cyclic ring from atoms N1, O1, O1a, N3, N4, and O2 (Figure 3b). The different coordination geometries around Dy^{III} ion in these compounds are probably responsible for the distinct magnetic behavior observed (see below).

Table 1. Crystallographic Data and Structure Refinement for Complexes 1 and 2

	1	2
formula	$C_{36}H_{40}Dy_2N_2O_{12}$	$C_{36}H_{44}Dy_2N_{10}O_{18}$
M_r	1017.70	1229.81
cryst size [mm]	0.20 × 0.18 × 0.16	0.19 × 0.18 × 0.16
color	pale yellow	red
cryst syst	triclinic	orthorhombic
space group	$P\bar{1}$	*Pnna*
T [K]	273(2)	273(2)
a [Å]	9.0109(4)	15.7438(10)
b [Å]	10.0056(5)	14.1723(9)
c [Å]	11.5680(6)	22.6961(14)
α [deg]	84.4320(10)	90
β [deg]	72.8300(10)	90
γ [deg]	66.5430(10)	90
V [Å^3]	913.88(8)	5064.09
Z	1	4
D_{calcd} [g cm^{-3}]	1.849	1.613
μ(Mo Kα) [mm^{-1}]	0.71073	0.71073
F(000)	498	2424.0
reflns collected	5083	32 268
unique reflns	3555	7169
R_{int}	0.0130	0.0762
parameters/restraints	236/0	301/6
GOF	1.053	1.051
R1 [$I > 2\sigma(I)$]	0.0249	0.0581
wR2 (all data)	0.0560	0.2015

MAGNETIC PROPERTIES

Direct Current (dc) Magnetism. Direct current (dc) magnetic susceptibility studies of poly crystalline samples (Figure 4) reveal a room-temperature $\chi_M T$ value of 27.1 cm^3 K mol^{-1} and 29.5 cm^3 K mol^{-1} for **1** and **2**, respectively, which is in agreement with the expected value of 28.34 cm^3 K mol^{-1} for two uncoupled Dy^{III} ions ($^6H_{15/2}$, $g = 4/3$). With decreasing the temperature, $\chi_M T$ product only displays a slight decrease to 26.0 cm^3 K mol^{-1} at 30 K for compound **1**, but a clear decrease to 22.7 cm^3 K mol^{-1} at 9 K in compound **2**, which may result from the depopulation of the Stark sublevels and/or significant magnetic anisotropy present in Dy^{III} systems. Furthermore, for compound **2**, $\chi_M T$ product shows a slight increase to 25.6 cm^3 K mol^{-1} at 2 K (Figure 4). In contrast, the product increases sharply to a maximum value of 36.2 cm^3 K mol^{-1} at 2 K in compound **1** (Figure 4), suggesting stronger intramolecular ferromagnetic interactions in **1** than those in **2**. As seen from Figure 4, compound **1** demonstrates stronger ferromagnetic

dx.doi.org/10.1021/ic400150f | Inorg. Chem. 2013, 52, 4587−4592

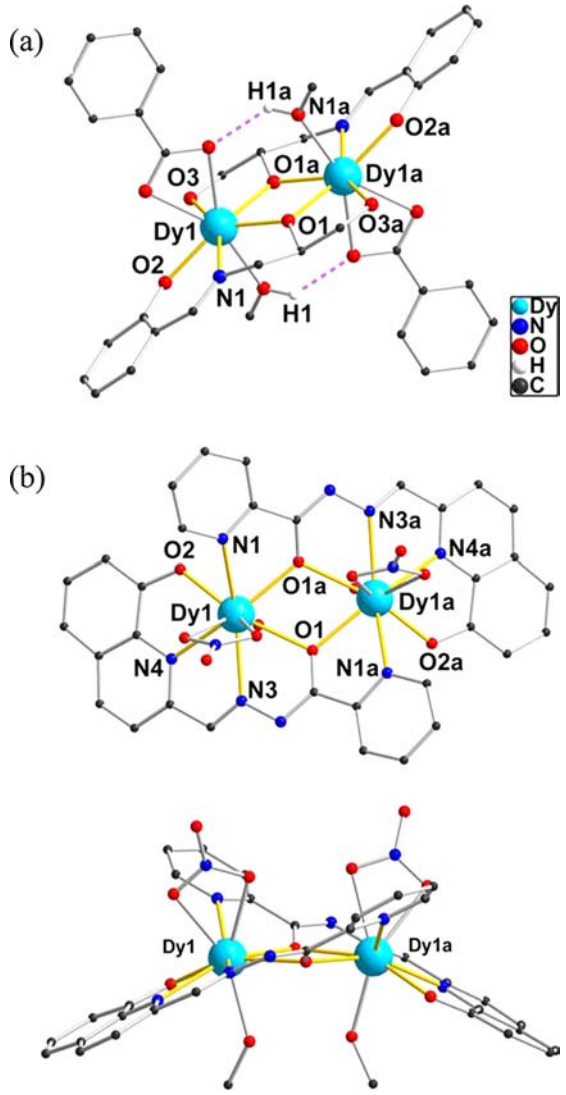

Figure 2. The crystal structures of compounds **1** (a) and **2** (b).

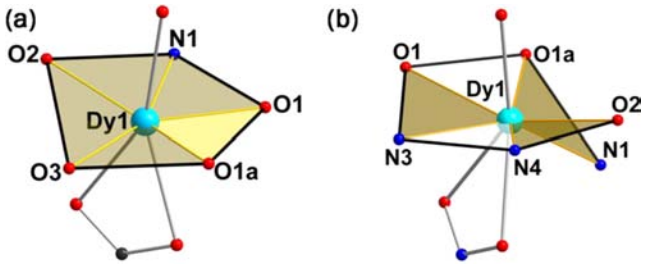

Figure 3. Left: Hula hoop-like geometry with the cyclic ring defined by the atoms N1, O1, O1a, O3, and O2 for compound **1**. Right: Broken hula hoop-like geometry for compound **2**.

interactions between metal centers, while weaker interactions are observed in compound **2**.

Magnetization (M) data for **1** and **2** were collected in the 0–70 kOe field range below 5 K. The *M* versus *H* data below 5 K (Figure S2) show a rapid increase in the magnetization at low magnetic fields, which is consistent with the presence of intramolecular ferromagnetic interactions. The magnetization eventually reaches the value of 12.0 μ_B for **1** (13.1 μ_B for **2**) at 2 K and 70 kOe. This value is lower than theoretical saturation value of 40 μ_B (4 × 10 μ_B), most likely due to the crystal field effect at the dysprosium(III) ion.[13] The nonsuperposition on a single mastercurve of the *M* versus *H*/*T* data (Figure 5) suggests the presence of a significant magnetic anisotropy and/or low-lying excited states in these systems.[28] In addition, it is worth mentioning that the *M* versus *H* data (Figure 4) give rise to a butterfly shaped hysteresis cycle at 1.65 K for compound **1**.

Alternating Current (ac) Magnetism. The temperature- (Figure 6, Figures S3 and Figure S4) and frequency-dependent (Figure S5) ac susceptibilities of compounds **1** and **2** were measured under zero dc field. At high temperature region (>5 K), out-of-phase (χ'') signals of compound **1** are observed with maxima at ∼15 K for 1488 Hz (Figure 6, left), revealing a slow relaxation of the magnetization that is typical for SMM behavior, which should arise from the strong axiality of Dy^{III} ion due to the hula hoop-like coordination geometry around it. At low temperatures (below 5 K), the temperature-dependent ac susceptibility shows almost negligible increase, suggesting the "freezing" of the spins by the anisotropy barriers and the effective suppression of zero-field tunneling of magnetization.[16] In contrast, no SMM behavior was observed under zero-field for compound **2**, as indicated by the temperature-dependent ac susceptibility data (Figure S4).

For compound **1**, the magnetization relaxation time (τ) is extracted from the frequency dependence measurements and is plotted as a function of 1/*T* (between 1.8 and 18 K) in Figure 7a. Remarkably, although the ac susceptibility was measured below the frequency of 1 Hz within the investigated temperature domain (Figure 7, inset), the frequency-independent peaks signaling the quantum tunneling region were not observed, indicating a slow quantum tunneling relaxation in compound **1**. At 1.9 K, the position of frequency-dependence peak is about 0.58 Hz, indicating a relaxation time of 274 ms ($\tau = 1/(2\pi\nu)$). Thus, the quantum tunneling time should be more than 274 ms, which is rather long in contrast to many reported Dy_2 SMMs.[29−31] At high temperature, the relaxation follows an Arrhenius-like behavior, affording a high spin reversal barrier of U_{eff} = 94 K with $\tau_0 = 2.1 \times 10^{-7}$ s. The Cole–Cole plots from the zero field measurements (Figure 7b) show a near symmetrical shape and can be fitted to the generalized Debye model, with α parameters below 0.19 between 1.9 and 15 K, indicating a very narrow distribution of relaxation times.

Structure–Property Relationship. To probe the structure–property relationship in compounds **1**, **2**, **3**, and **4**, some crucial parameters of structure, including bond lengths of Dy–O in Dy_2O_2 core (d_{Dy-O}(core)), the average bond lengths of Dy–O/N at the cyclic ring of hula hoop ($d_{average}$), Dy···Dy distances, and Dy–O–Dy angles have been listed in Table 2. It is noteworthy that all compounds have similar Dy–O–Dy angles (>110°), but compound **1** displays the shortest Dy–O bonds in Dy_2O_2 cores of four compounds, thus leading to the shortest Dy···Dy distance, further confirming the occurrence of stronger intramolecular interactions between metal ions, as reflected by Figure 4. Here, the strong interactions of compound **1** should be as a result of the more strongly negative charge of alkoxide group of ligand H_3L_1 as compared to that of the hydrazone-O. Further, the shortest average bond length of Dy–O/N at the position of cyclic ring was observed in compound **1**, suggesting the formation of a strong ligand field on the local Dy^{III} sites of compound **1**. In addition, the weakest ferromagnetic interactions were observed in compound

dx.doi.org/10.1021/ic400150f | Inorg. Chem. 2013, 52, 4587–4592

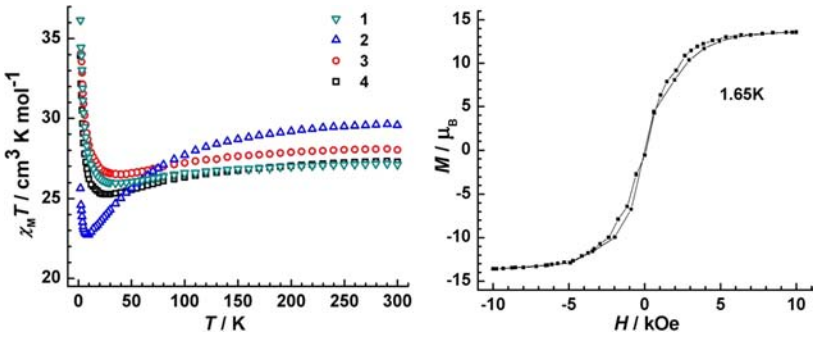

Figure 4. Left: Plots of $\chi_M T$ versus T for compounds **1**, **2**, **3**, and **4**. Right: M versus H data of **1** at 1.65 K emphasizing the butterfly shaped hysteresis.

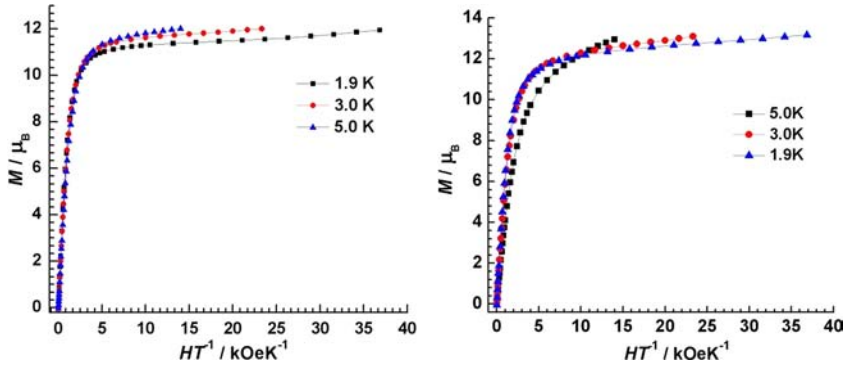

Figure 5. M versus H/T plots between 1.9, 3.0, and 5 K for compounds **1** (left) and **2** (right). The solid lines are a guide for the eyes.

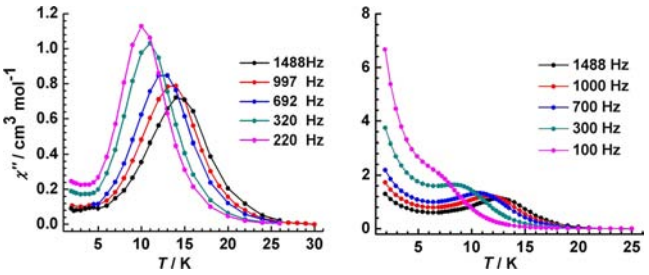

Figure 6. Temperature dependence of the out-of-phase (χ'') ac susceptibility of compounds **1** (left) and **4** (right). Solid lines are guides for the eyes.

2 (Figure 4), possibly resulting from the large Dy···Dy separation induced by the bent of ligand H_2L_2.

Table 2. Some Crucial Structural Parameters for Compounds 1, 2, 3, and 4

	compound			
	1	**2**	**3**	**4**
d_{Dy-O} (Å)	2.295(2)	2.463(5)	2.334(8)	2.348(1)
	2.261(0)	2.370(5)	2.333(3)	2.318(6)
$d_{average}$ (Å)	2.333(4)		2.370(8)	2.355(1)
Dy···Dy (Å)	3.769(9)	4.074(3)	3.864(4)	3.825(8)
Dy−O−Dy	111.67°	114.88°	112.20°	110.12°

Among the four compounds, both **1** and **4** show similar crystal structure and ac magnetic properties, and some surprising results can be grasped through the comparison of them. At high temperature (>5 K), ac susceptibility curves demonstrate the higher blocking temperature in compound **1** than that in compound **4** (Figure 6), which should arise from

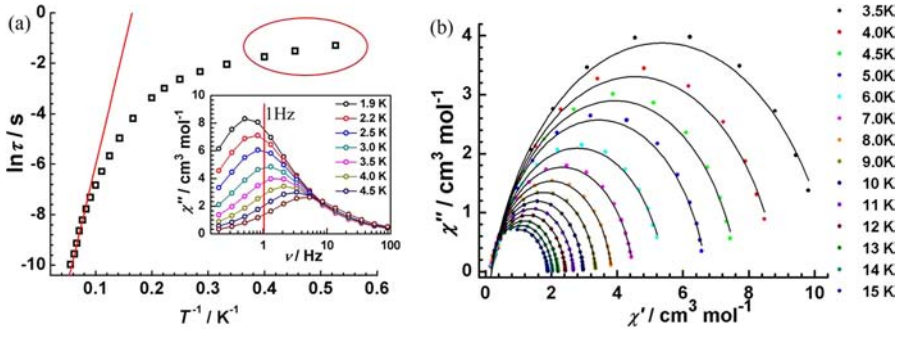

Figure 7. (a) Fitting of the relaxation time (τ) from frequency dependence of the out-of-phase (χ'') parts of the ac susceptibility using Arrhenius law for compound **1** (inset: frequency dependence of χ'' of the ac susceptibility below 100 Hz). (b) Cole−Cole plots under zero-dc field for compound **1**. The solid lines indicate the fits using a generalized Debye model.

dx.doi.org/10.1021/ic400150f | Inorg. Chem. 2013, 52, 4587−4592

the stronger ligand field of compound **1**. Notably, more obvious differences are observed at low temperature (<5 K) for compounds **1** and **4**, where compound **1** shows very weak quantum tunneling. This should be ascribed to the strong intramolecular interactions modulated by alkoxide-O bridges as well as strong ligand field in compound **1**.[16,32] As for compound **2**, the obvious disparity in magnetic dynamics from other compounds should mainly result from the broken coordination geometry, thus leading to the fast quantum tunneling from more transverse anisotropy.

CONCLUSION

Two novel Dy_2 compounds (**1** and **2**) have been assembled from different types of ligands (H_3L_1 and H_2L_2). Compound **1** with H_3L_1 represents the rare alkoxide-O bridged Dy_2 complex and displays the hula hoop-like coordination geometry around each Dy^{III} ion, thus leading to the typical SMM behavior in combination of the stronger ferromagnetic interactions between Dy^{III} ions. The distorted coordination geometry around Dy^{III} ion and much weaker interactions observed in compound **2** due to the introduction of bent H_2L_2 result in the disappearance of SMM behavior. Our simple comparative investigations may shed light on the structure−property relationship of lanthanide-based SMMs, which is crucial to the advancement of single-molecule data storage and processing technologies. It should be pointed out that the magneto-structural relation analysis in Dy_2 system has progressed quantitatively thanks to the ab initio calculations developed by Liviu Chibotaru et al. as successfully employed in Dy_2[31,33] and $Dy_2Co^{III}_2$.[34] In this regard, further investigations including ab initio calculations and magnetic dilution are required to elucidate the mechanisms operating in our compounds.

ASSOCIATED CONTENT

Supporting Information

Crystal structures and magnetic measurement (Figures S1−S7). X-ray crystallographic data in CIF format (CCDC 894094 (**1**) and 894095 (**2**)). This material is available free of charge via the Internet at http://pubs.acs.org.

AUTHOR INFORMATION

Corresponding Author

*E-mail: tang@ciac.jl.cn.

Notes

The authors declare no competing financial interest.

ACKNOWLEDGMENTS

We thank the National Natural Science Foundation of China (Grants 91022009, 21241006, and 21221061) for financial support.

REFERENCES

(1) Sessoli, R.; Gatteschi, D.; Caneschi, A.; Novak, M. A. *Nature* **1993**, *365*, 141.
(2) Hussain, B.; Savard, D.; Burchell, T. J.; Wernsdorfer, W.; Murugesu, M. *Chem. Commun.* **2009**, 1100.
(3) Anwar, M. U.; Thompson, L. K.; Dawe, L. N.; Habib, F.; Murugesu, M. *Chem. Commun.* **2012**, *48*, 4576.
(4) Wernsdorfer, W.; Aliaga-Alcalde, N.; Hendrickson, D. N.; Christou, G. *Nature* **2002**, *416*, 406.
(5) Dei, A.; Gatteschi, D. *Angew. Chem., Int. Ed.* **2011**, *50*, 11852.
(6) Blagg, R. J.; Muryn, C. A.; McInnes, E. J. L.; Tuna, F.; Winpenny, R. E. P. *Angew. Chem., Int. Ed.* **2011**, *50*, 6530.
(7) Rinehart, J. D.; Fang, M.; Evans, W. J.; Long, J. R. *J. Am. Chem. Soc.* **2011**, *133*, 14236.
(8) Benelli, C.; Gatteschi, D. *Chem. Rev.* **2002**, *102*, 2369.
(9) Rinehart, J. D.; Long, J. R. *Chem. Sci.* **2011**, *2*, 2078.
(10) Habib, F.; Long, J.; Lin, P.-H.; Korobkov, I.; Ungur, L.; Wernsdorfer, W.; Chibotaru, L. F.; Murugesu, M. *Chem. Sci.* **2012**, *3*, 2158.
(11) Sorace, L.; Benelli, C.; Gatteschi, D. *Chem. Soc. Rev.* **2011**, *40*, 3092.
(12) Tuna, F.; Smith, C. A.; Bodensteiner, M.; Ungur, L.; Chibotaru, L. F.; McInnes, E. J. L.; Winpenny, R. E. P.; Collison, D.; Layfield, R. A. *Angew. Chem., Int. Ed.* **2012**, *51*, 6976.
(13) Guo, Y.-N.; Chen, X.-H.; Xue, S.; Tang, J. *Inorg. Chem.* **2011**, *50*, 9705.
(14) Ishikawa, N.; Sugita, M.; Ishikawa, T.; Koshihara, S.-y.; Kaizu, Y. *J. Am. Chem. Soc.* **2003**, *125*, 8694.
(15) Wang, H.; Wang, K.; Tao, J.; Jiang, J. *Chem. Commun.* **2012**, *48*, 2973.
(16) Guo, Y.-N.; Xu, G.-F.; Wernsdorfer, W.; Ungur, L.; Guo, Y.; Tang, J.; Zhang, H.-J.; Chibotaru, L. F.; Powell, A. K. *J. Am. Chem. Soc.* **2011**, *133*, 11948.
(17) Guo, Y.-N.; Chen, X.-H.; Xue, S.; Tang, J. *Inorg. Chem.* **2012**, *51*, 4035.
(18) Bhunia, A.; Gamer, M. T.; Ungur, L.; Chibotaru, L. F.; Powell, A. K.; Lan, Y.; Roesky, P. W.; Menges, F.; Riehn, C.; Niedner-Schatteburg, G. *Inorg. Chem.* **2012**, *51*, 9589.
(19) Bharara, M. S.; Strawbridge, K.; Vilsek, J. Z.; Bray, T. H.; Gorden, A. E. V. *Inorg. Chem.* **2007**, *46*, 8309.
(20) Nayak, S.; Nayek, H. P.; Dehnen, S.; Powell, A. K.; Reedijk, J. *Dalton Trans.* **2011**, *40*, 2699.
(21) Zhang, S.-Y.; Chen, W.-Q.; Hu, B.; Chen, Y.-M.; Li, W.; Li, Y. *Inorg. Chem. Commun.* **2012**, *16*, 74.
(22) Boudreaux, E. A.; Mulay, L. N. *Theory and Applications of Molecular Paramagnetism*; John Wiley & Sons: New York, 1976.
(23) Sheldrick, G. M. *Acta Crystallogr., Sect. A* **2008**, *64*, 112.
(24) Leng, J.-D.; Liu, J.-L.; Zheng, Y.-Z.; Ungur, L.; Chibotaru, L. F.; Guo, F.-S.; Tong, M.-L. *Chem. Commun.* **2013**, *49*, 158.
(25) Yang, P.-P.; Gao, X.-F.; Song, H.-B.; Zhang, S.; Mei, X.-L.; Li, L.-C.; Liao, D.-Z. *Inorg. Chem.* **2010**, *50*, 720.
(26) Chen, Y.-H.; Tsai, Y.-F.; Lee, G.-H.; Yang, E.-C. *J. Solid State Chem.* **2012**, *185*, 166.
(27) Wang, Y.-X.; Shi, W.; Li, H.; Song, Y.; Fang, L.; Lan, Y.; Powell, A. K.; Wernsdorfer, W.; Ungur, L.; Chibotaru, L. F.; Shen, M.; Cheng, P. *Chem. Sci.* **2012**, *3*, 3366.
(28) Lin, P.-H.; Sun, W.-B.; Yu, M.-F.; Li, G.-M.; Yan, P.-F.; Murugesu, M. *Chem. Commun.* **2011**, *47*, 10993.
(29) Lin, P.-H.; Burchell, T. J.; Clérac, R.; Murugesu, M. *Angew. Chem., Int. Ed.* **2008**, *47*, 8848.
(30) Xu, G. F.; Wang, Q. L.; Gamez, P.; Ma, Y.; Clérac, R.; Tang, J. K.; Yan, S. P.; Cheng, P.; Liao, D. Z. *Chem. Commun.* **2010**, *46*, 1506.
(31) Long, J.; Habib, F.; Lin, P.-H.; Korobkov, I.; Enright, G.; Ungur, L.; Wernsdorfer, W.; Chibotaru, L. F.; Murugesu, M. *J. Am. Chem. Soc.* **2011**, *133*, 5319.
(32) Sulway, S. A.; Layfield, R. A.; Tuna, F.; Wernsdorfer, W.; Winpenny, R. E. P. *Chem. Commun.* **2012**, *48*, 1508.
(33) Habib, F.; Lin, P.-H.; Long, J.; Korobkov, I.; Wernsdorfer, W.; Murugesu, M. *J. Am. Chem. Soc.* **2011**, *133*, 8830.
(34) Langley, S. K.; Chilton, N. F.; Ungur, L.; Moubaraki, B.; Chibotaru, L. F.; Murray, K. S. *Inorg. Chem.* **2012**, *51*, 11873.